# Soil lacunar factor and reference shrinkage

*V.Y. Chertkov*

Faculty of Civil and Environmental Engineering, Technion, Haifa 32000, Israel

A b s t r a c t. At sufficiently small soil clay content, the clay contributing to the soil aggregates usually contains so-called lacunar pores that are essentially larger than the clay matrix pores. A recently introduced parameter, the soil lacunar factor, determines the volume fraction of the clay matrix pore decrease at shrinkage that is transformed to the lacunar pore volume increase inside aggregates. The lacunar factor essentially influences the soil shrinkage and is a fundamental soil property that can be found independently of a measured shrinkage curve. The aim of this work was to theoretically derive and experimentally validate an expression to estimate the soil lacunar factor through the actual soil clay content and critical soil clay content (when the actual soil clay content is higher than critical one the lacunar pores lack). To validate the approach the available data of sixteen soils were used.

K e y w o r d s: soil aggregates, soil physical properties, soil reference shrinkage, lacunar factor, aggregate surface layer

## INTRODUCTION

The shrinkage curve is one of the key soil characteristics in both agricultural and civil engineering applications. The contemporary methods of its measurement are known (Braudeau *et al*., 1999, 2004; Sander and Gerke, 2007; Tariq and Durnford, 1993). However, the possibility of predicting an observed soil shrinkage curve in the meaning of physical prediction *ie* from a finite number of physical soil parameters that are measured or estimated independently of the soil shrinkage, is so far lacking. Available models of the soil shrinkage with all essential differences between them are reduced to curve-fitting to relevant experimental soil shrinkage data (Cornelis *et al*., 2006; Giraldez *et al.*, 1983; Groenevelt and Bolt, 1972; Groenevelt and Grant, 2001; Olsen and Haugen, 1998; Peng and Horn, 2005). The authors use parameters (from 3 to 11 depending on the model) of some mathematical approximation (different for different models) of a shrinkage curve in the fitting. At least a part of these parameters in

each of the models has no clear physical meaning and can only be found by fitting. As a consequence, although the models can be practically useful for applications in civil engineering, soil technology, and water management, their possibilities from the viewpoint of advancement in physical understanding and knowledge of the links between soil structure and soil shrinkage as a function of the structure, are in the best case, limited. In addition, the shrinkage curve of a soil is non-single valued since the crack volume contribution to the shrinking soil volume depends on sampling, sample preparation, sample size, and drying regime (Braudeau *et al*., 1999; Cabidoche and Ruy, 2001; Crescimanno and Provenzano, 1999; McGarry and Daniels, 1987; Yule and Ritchie, 1980a,b).

Recently a new approach to physical prediction of soil shrinkage (without fitting) was proposed (Chertkov, 2007a, b, c; 2008a). This approach investigated the reference shrinkage curve that, by definition, corresponds to shrinkage without inter-aggregate cracking and for this reason can be predicted in a single-valued manner. The approach derives the reference shrinkage curve of a soil from the shrinkage curve of a clay contributing to the soil and two new features of the intra-aggregate soil structure:
– the existence and dewatering of a deformable, but non-shrinking aggregate surface layer (interface layer),
– the existence and volume increase of intra-aggregate lacunar pores at soil shrinkage.

The interface layer exists at any soil clay content. Its mean thickness increases as clay content decreases. The lacunar pores exist at a clay content lower than a critical value. The derivation of the reference shrinkage curve leads to the understanding of the origin of the shape of a soil shrinkage curve and can be used in estimating the contribution of the crack volume to the soil shrinkage curve (Chertkov, 2008b, c), the soil hydraulic properties, and in other applications as

---

Corresponding author's e-mail: vychert@ymail.com

well as in preparing the soil with *a priori* given shrinkage properties. The reference shrinkage curve is determined by a number of physical soil characteristics that can be measured independently of the shrinkage curve. Among them there are two new characteristics:

– the ratio of the aggregate solid mass to the solid mass of the intra-aggregate matrix (*K* ratio),

– the lacunar factor that characterizes the rate of lacunar pore volume change with water content (*k* factor).

Both these characteristics have a clear physical meaning and can be easily obtained in two ways - as fitting parameters (the traditional way in civil engineering, soil science, and hydrology) and immediately from the geometrical characteristics of a measured shrinkage curve (Chertkov, 2007c). The accordance between the *K* and *k* values obtained by the above two ways means that these parameters are fundamental soil characteristics. However, of the special interest is the possibility of estimating these physical soil characteristics based on the soil structure and independently of an experimental shrinkage curve. Such consideration, as applied to the *K* ratio, was recently undertaken (Chertkov, 2008d).

The aim of this work is to propose an approach for estimating the *k* factor at any sufficiently low soil clay content through other soil characteristics.

For the model validation available data on the properties and shrinkage curves of sixteen soils were used. A part of these soils was earlier used in the validation of the reference shrinkage curve approach (Chertkov, 2007c). The others are also used in this work, in addition to the above major objective, as supplemental confirmation of the reference shrinkage curve approach.

### THEORY

In the case of a sufficiently small clay content (the specification see below) the soil lacunar factor, *k* is defined as the fraction of the increment of the clay matrix pore volume at shrinkage, $du_{cp}<0$ that is transformed to the corresponding increment of the lacunar pore volume inside aggregates, $du_{lp}>0$ (Fig. 1b). That is, by definition (Chertkov, 2007c; 2008a):

$$du_{lp} = -k \, du_{cp}, \qquad 0 \le k = \text{const} < 1. \qquad (1)$$

Here $u_{cp}$ and $u_{lp}$ are the relative clay pore ('cp' index) and lacunar pore ('lp' index) volume within the limits of the intra-aggregate matrix (Fig. 1b) ('relative' means the ratio of a corresponding volume to that of the intra-aggregate matrix at the liquid limit). The following result (Chertkov, 2007c; 2008a) is essential: that the *k* factor, by definition connected with the variation of the intra-aggregate structure of a soil at shrinkage, determines the slope, *S* of the reference shrinkage curve in the basic shrinkage area as:

$$S = (1-k)/\rho_w , \qquad (2)$$

where $\rho_w$ is the water density. Equation (2) gives the simple connection between the immediately observed (macro) parameter of soil shrinkage (*S*) and (micro) parameter of the intra-aggregate structure (*k*).

All soils can be divided into two groups with the clay content, *c* higher and lower than some critical value, *c\** (Chertkov, 2007a, c; 2008a). The latter depends on the shrinkage characteristics of the contributive clay and the inter-grain porosity of the silt and sand component (with smooth grain-size distribution according to the intersecting surfaces approach from Chertkov (2005)) contributing to the soil when the grains are in (imagined) contact (see below). By definition the critical value *c=c\** corresponds to such clay content that is necessary and sufficient to fill in the pores between the contacting silt and sand grains contributing to the soil aggregates in the oven-dried state. It is obvious that at *c>c\** (Fig. 1a) the silt and sand grains cannot be in contact (and even more so at water content *W>0*), and the space between them is filled in with clay. In this case (Fig. 1a) there are no lacunar pores and the lacunar factor *k=0* (since $du_{lp}=0$ in Eq.(1)). We are interested in the opposite case of *c<c\** when the space between contacting silt and sand grains inside aggregates is not totally filled in with clay and contains lacunar pores. However, in fact, at *c<c\** the grain arrangement with total contact inside aggregates is neither the only possible nor the most probable case. In real soils many silt and sand grains in the intra-aggregate matrix do not touch even at *c<c\** (Fig. 1b). This means that at a given clay content the soil can have different lacunar porosity. The lacunar factor, *k* determines the transition from the initial
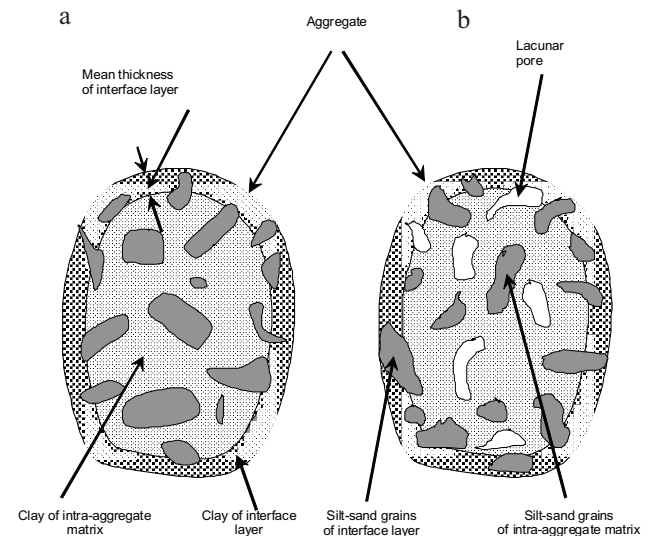


**Fig. 1.** Illustrative scheme of the internal structure of soil aggregates at a clay content (the modified Fig. 2 from Chertkov, 2008a): a – *c>c\**, without lacunar pores; b – *c<c\**, with lacunar pores and possible non-totally contacting silt and sand grains. *c\** is the critical soil clay content.

(relative) volume of lacunar pores at maximum soil swelling, $u_{lph}$ to the final (relative) volume of the lacunar pores at maximum shrinkage, $u_{lpz}$ ($>u_{lph}$) (indices 'h' and 'z' correspond to the maximum swelling and shrinkage, respectively) as (Chertkov, 2007c):

$$u_{lph}=u_{lpz}-k(1-u_S)(v_h-v_z), \qquad (3)$$

where: $v_h$ and $v_z$ are the relative volume of the contributive clay at the maximum swelling and in the oven-dried state, respectively; $u_S$ is the relative volume of the silt and sand component of the soil.

Our objective is to estimate the $k$ factor of a soil from its characteristics. One could use Eq. (3) to estimate the $k$ value of a concrete soil if the $u_{lph}$ and $u_{lpz}$ values of the soil are known. However, the $k$ lacunar factor in itself does not depend on the initial ($u_{lph}$) and final ($u_{lpz}$) lacunar pore volumes that, as noted above, can be different at a given $k$. Note that the lacunar pores develop inside aggregates. For this reason and according to its physical meaning, the $k$ value can only depend (except for the soil clay content, $c$) on the characteristics of the intra-aggregate matrix (Fig. 1b) such as those of the contributive clay – the relative volume of clay solids, $v_s$ and oven-dried clay, $v_z$ (Chertkov, 2000, 2003) as well as the porosity, $p$ of contributive silt and sand grains when they are in the state of (imagined) contact. These characteristics enter the expression for $c^*$ (Chertkov, 2007a) as:

$$c^*=[1+(v_z/v_s)(1/p-1)]^{-1}. \qquad (4)$$

For this reason we assume that at $c<c^*$ (Fig. 1b) the soil lacunar factor $k$ as a function of the clay content, $c$ is a universal function $k(c/c^*)$ of the $c/c^*$ ratio at $0<c/c^*<1$ (at $c/c^*>1$ $k\equiv0$, Fig. 1a). With that, the $k(c/c^*)$ function meets the following obvious physical conditions (Fig. 2):

$$k(0)=1, k'(0)=0, k(c/c^*\rightarrow1-\varepsilon)\rightarrow0, k'(c/c^*\rightarrow1-\varepsilon)\rightarrow-\infty. \qquad (5)$$

Indeed, there is the qualitative difference between the cases of Fig.1a, b. For this reason, at the transition from $c/c^*=1+\varepsilon$ to $c/c^*=1-\varepsilon$ ($\varepsilon$ is an infinitesimal value, Fig. 2) $k$ changes dramatically from zero (for the case of Fig.1a) to a very small, but finite value (for the case of Fig.1b). This is why the two last conditions of Eq. (5) take place. Note that for real soils even with a small clay content, $c$ the $k$ values very close to unity are practically unobservable because at any clay content the $c/c^*$ ratio usually exceeds $\sim$0.5 (Fig. 2). This means that at least the second derivative of the $k(c/c^*)$ function at $c/c^*\rightarrow0$ is also zero (Fig. 2) as:

$$k''(0)=0. \qquad (6)$$

The jump-like change of $k(c/c^*)$ at transition from $c/c^*>1$ to $c/c^*<1$ also means that in addition to $k'(c/c^*\rightarrow1-\varepsilon)\rightarrow-\infty$ at least:

$$k''(c/c^*\rightarrow1-\varepsilon)\rightarrow-\infty. \qquad (7)$$
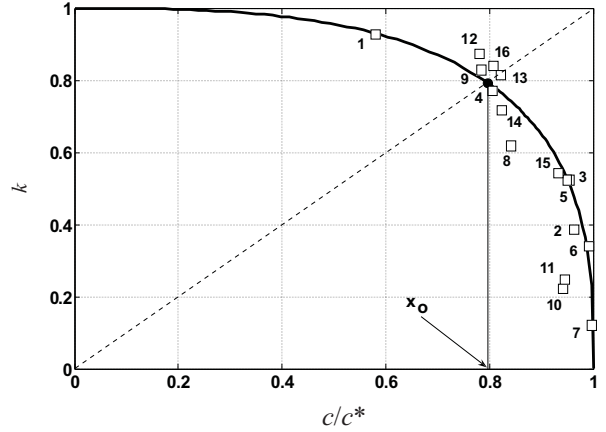


**Fig. 2.** The solid curve simultaneously illustrates: a – the qualitative view of $k(c/c^*)$ dependence that flows out of the physical heuristic considerations before its derivation, b – the analytical dependence of $k(c/c^*)$ (Eq. (14)) derived in the work. White squares show experimental data from sixteen soils (the numbers refer to soils shown in Tables 1 and 2).

Then at small $c/c^*$ values one can approximate $k(c/c^*)$ as (Fig. 2):

$$k\cong1-D(c/c^*)^3, \qquad c/c^*<<1 \qquad (D>0), \qquad (8)$$

if the first two conditions of Eq. (5) and condition of Eq. (6) are taken into account. Similarly, using the last two conditions of Eq. (5) and condition of Eq. (7) one can approximate the $c/c^*$ ratio as a function of $k$ at small $k$ values as (Fig. 2):

$$c/c^*\cong1-D'k^3, \qquad k<<1 \qquad (D'>0). \qquad (9)$$

We replace Eq. (8) with:

$$k\cong[1-(c/c^*)^3]^D, \qquad c/c^*<<1, \qquad (10)$$

that coincides with Eq. (8) at $c/c^*<<1$. Similarly, we replace Eq. (9) with:

$$c/c^*\cong(1-k^3)^{D'}, \qquad k<<1, \qquad (11)$$

that coincides with Eq.(9) at $k<<1$. Now using Eq.(11) one can write:

$$k\cong[1-(c/c^*)^{1/D'}]^{1/3}, \qquad 1-c/c^*<<1. \qquad (12)$$

The approximations of $k(c/c^*)$ in the vicinity of $c/c^*=0$ (Eq. (10) and Fig. 2) and $c/c^*=1-\varepsilon$ (Eq. (12) and Fig. 2) lead to heuristic considerations about $k(c/c^*)$ dependence in the intermediate area and can obviously be used in such an area. Thus, we assume that (Fig. 2):

$$k=\begin{cases} \left[1-(c/c^*)^3\right]^D, & 0<c/c^*<x_o \\ \left[1-(c/c^*)^{1/D'}\right]^{1/3}, & x_o<c/c^*<1 \end{cases}. \qquad (13)$$

To find the $x_o$, $D$ and $D'$ values we have the conditions of continuity and smoothness of $k(c/c^*)$ at $c/c^*=x_o$ (Fig. 2). In addition the $k(c/c^*)$ expression should be a single-valued one in the range of $0<c/c^*<1$. The simple calculation based on these three conditions results in $D=D'=0.3286$ and $x_o=0.795$. Thus, finally (Fig. 2):

$$k = \begin{cases} \left[1-(c/c^*)^3\right]^{0.3286}, & 0<c/c^*<0.795 \\ \left[1-(c/c^*)^{1/0.3286}\right]^{1/3}, & 0.795<c/c^*<1 \end{cases} \quad (14)$$

The curve of $k(c/c^*)$ from Eq. (14) (Fig. 2) is symmetrical with respect to the diagonal (dashed line in Fig. 2). That is, the $c/c^*$ ratio as a function of $k$, mathematically coincides with the $k(c/c^*)$ function from Eq. (14). One can also see that the expressions for $k(c/c^*)$ at $0<c/c^*<0.795$ and $0.795<c/c^*<1$ differ only a little because $1/3\cong0.3286$. Practically, one can use the simple expression $k\cong[1-(c/c^*)^3]^{1/3}$ in the total range $0<c/c^*<1$ and $0<k<1$, but the presentation of Eq. (14) is still more theoretically substantiated. The data on $k(c/c^*)$ dependence and comparison between them and the theoretical presentation (Eq. (14)) will be considered below.

## MATERIALS AND METHODS

To confirm the model in this work we are interested in independent findings of the soil lacunar factor, $k$ and $c/c^*$ ratio that possibly cover a wider area within the limits of the formal ranges of $0<k<1$ and $0<c/c^*<1$. One soil (with $c/c^*<1$) gives one point on the ($c/c^*$, $k$) plane. For that soil we need data or estimates of $k$, $c$, and $v_s$, $v_z$, $p$ to find $c^*$ (Eq. (4)). Data that could be attracted for checking the model are available in the literature. We used data for sixteen soils (with $c/c^*<1$) to extract the corresponding $k$, $c$, $v_s$, $v_z$, and $p$ value sets: seven soils from Braudeau *et al.* (2005), seven soils from Boivin *et al.* (2006), and two soils from Braudeau and Mohtar (2004). These soils are indicated and numbered in Table 1. The primary data for each soil that we used included the experimental shrinkage curve, soil clay content ($c$), and soil solid density ($\rho_s$). All characteristics of the sixteen soils given in Table 1 (except for data on $c$ and $\rho_s$ that were immediately taken from the above three references) were estimated as a result of the analysis of the experimental shrinkage curve for each soil. The analysis was recently described in detail (Chertkov, 2007a, c) and is destined for construction or prediction of the reference shrinkage curve using a number of physical soil characteristics (the latter, in principle, can be found independently of a shrinkage curve). In particular, the above data on the shrinkage curves for the seven soils from Braudeau *et al.* (2005) have already been analyzed (Chertkov, 2007c). All characteristics of these soils in Tables 1 and 2 that will be used for aims of this work,

reproduce estimates from Chertkov (2007c). The data for the other nine soils were analyzed for the first time. As examples, Figs 3 and 4 show the predicted curves and shrinkage curve data for two soils of these nine. To predict the reference shrinkage curve, one needs (Chertkov, 2007c):

– the oven-dried specific volume, $Y_z$;
– maximum swelling (gravimetric) water content, $W_h$;
– mean solid density, $\rho_s$;
– soil clay content, $c$;
– oven-dried structural porosity, $P_z$;
– the ratio of aggregate solid mass to solid mass of intra-aggregate matrix, $K$;
– the lacunar factor, $k$;
– water content $W_h^*$ with a displacement relative to $W_h$ that is similar to the displacement of the true saturated line relative to pseudo-one.

The $Y_z$, $W_h$, and $W_h^*$ values were estimated from the initial and final points of shrinkage (Figs 3 and 4). In estimating the structural porosity, $P_z$ we took into account that $P_z$ differs of zero if the shrinkage curve has a horizontal section at water content $W>W_h$, that is higher than the maximum swelling point (Chertkov, 2007c). The size of the section determines the specific volume of the structural (inter-aggregate) pores, $U_s$ and $P_z=U_s/Y_z$. If $U_s=0$ $P_z=0$ (as in Figs 3 and 4). In this work $K$ was estimated using its definition as the $W_h/w_h'$ ratio (Chertkov, 2008d). Finally, $k$ was estimated as $1-S\rho_w$ (Eq. (2)) where $S$ is the slope of the experimental shrinkage curve in the basic shrinkage area (Figs 3 and 4 at $W_n<W<W_s$).

Parameters $v_s$, $v_z$, $u_z$, and $u_S$ (Table 2) were also estimated ($u_z$ is the oven-dried relative volume of the intra-aggregate matrix; $u_S$ is the relative volume of the non-clay solids) in the course of the construction of the reference shrinkage curve for a soil (Figs 3 and 4) according Chertkov approach (2007a, c). These parameters enable one to estimate the $p$ and then $c^*$ values as follows. The porosity $p$ of the contributive silt and sand grains in the state of (imagined) contact is an independent soil property that can be measured in the soil analysis. However, for the soils under consideration the direct data on $p$ were unavailable. For this reason we approximated the $p$ value of a soil by some average, $p_{av}$ as:

$$p_{av}=(p_{max}+p_{min})/2 \quad (15)$$

from the upper ($p_{max}$) and lower ($p_{min}$) boundaries of $p$ at given $v_s$, $v_z$, $u_z$, $u_S$, and $c$ (Chertkov, 2007c) as:

$$p_{max}=1-u_S/u_z, \quad p_{min}=[1+(v_s/v_z)(1/c-1)]^{-1}. \quad (16)$$

Then the critical clay content, $c^*$ was estimated from Eq. (4) with $p\cong p_{av}$. Table 2 shows the $p_{max}$, $p_{min}$, $p_{av}$, $c^*$, and $c/c^*$ values that were found for the sixteen soils. In connection with the above estimation of the $p\cong p_{av}$ value, it is worth noting that in many cases (Table 2) the range $p_{min}<p<p_{max}$ is quite narrow, that is $(p_{max}-p_{min})/p_{min}<<1$.

**T a b l e  1.** Input parameters of the sixteen soils for reference shrinkage curve prediction

| Points No. in Figs 2, 5 | Data source | Input parameters* | | | | | | | | |
|---|---|---|---|---|---|---|---|---|---|---|
| | | $Y_z$ (dm³ kg⁻¹) | $W_h$ (kg kg⁻¹) | $\rho_s$ (kg dm⁻³) | $c$ | $P_z$ | $K$ | $k$ | $W_h^*$ kg kg⁻¹ | $\delta$ (%) |
| 1 | Braudeau *et al.* (2005, Fig. 3), ferruginous soil, A horizon | 0.642 | 0.200 | 2.337 | 0.065 | 0 | 3 | 0.929 | 0.217 | 0.06 |
| 2 | As above, B1 horizon | 0.692 | 0.235 | 2.337 | 0.340 | 0.038 | 1.894 | 0.387 | 0.255 | 0.12 |
| 3 | As above, B2 horizon | 0.688 | 0.211 | 2.337 | 0.353 | 0.051 | 1.538 | 0.524 | 0.239 | 0.20 |
| 4 | As above, AB horizon | 0.682 | 0.229 | 2.337 | 0.187 | 0 | 2.499 | 0.771 | 0.266 | 0.08 |
| 5 | As above, ferralitic soil, A horizon | 0.878 | 0.543 | 2.608 | 0.523 | 0 | 1.892 | 0.523 | 0.553 | 0.22 |
| 6 | As above, ferralitic soil, B1 horizon | 0.696 | 0.351 | 2.608 | 0.648 | 0 | 1.433 | 0.340 | 0.351 | 0.23 |
| 7 | As above, ferralitic soil, B2 horizon | 0.731 | 0.362 | 2.608 | 0.648 | 0.031 | 1.424 | 0.121 | 0.362 | 0.33 |
| 8 | Boivin *et al.* (2006, Fig. 2a), Cambisol | 0.687 | 0.326 | 2.660 | 0.170 | 0 | 1.031 | 0.620 | 0.365 | 0.86 |
| 9 | As above (Fig. 2b), Cambisol | 0.674 | 0.285 | 2.660 | 0.140 | 0 | 1.035 | 0.829 | 0.321 | 0.30 |
| 10 | As above (Fig. 2c), Vertisol | 0.598 | 0.298 | 2.660 | 0.460 | 0.158 | 1.153 | 0.223 | 0.298 | 1.26 |
| 11 | As above (Fig. 2d), Vertisol | 0.581 | 0.321 | 2.650 | 0.510 | 0.130 | 1.043 | 0.248 | 0.321 | 2.96 |
| 12 | As above (Fig. 2e), Fluvisol | 0.558 | 0.142 | 2.660 | 0.090 | 0 | 2.709 | 0.875 | 0.184 | 0.02 |
| 13 | As above (Fig. 5a), Cambisol | 0.720 | 0.296 | 2.660 | 0.150 | 0 | 1.046 | 0.815 | 0.362 | 0.29 |
| 14 | As above (Fig. 5b), Fluvisol | 0.663 | 0.272 | 2.660 | 0.170 | 0 | 2.216 | 0.719 | 0.304 | 0.40 |
| 15 | Braudeau and Mohtar (2004, Fig.3), Booro Borotou Seq., Ivory Coast, sample T340 | 0.659 | 0.249 | 2.660 | 0.374 | 0 | 1.527 | 0.543 | 0.302 | 0.30 |
| 16 | As above, sample T740 | 0.604 | 0.205 | 2.660 | 0.229 | 0 | 1.548 | 0.840 | 0.240 | 0.14 |

*Oven-dried specific volume ($Y_z$), maximum swelling water content ($W_h$), mean solid density ($\rho_s$), soil clay content ($c$), oven-dried structural porosity ($P_z$), aggregate/intra-aggregate mass ratio ($K$), lacunar factor ($k$), and water content ($W_h^*$) that corresponds to filling in lacunar pores. Maximum relative difference ($\delta$) between predicted and measured volume shrinkage.

**T a b l e  2.** The $k$ factor and $c/c^*$ ratio with parameters used to estimate $c/c^*$

| Points No. in Figs 2, 5 | $k$ | $c/c^*$ | Parameters[1] | | | | | | | | |
|---|---|---|---|---|---|---|---|---|---|---|---|
| | | | $c$ | $v_s$ | $v_z$ | $u_z$ | $u_S$ | $p_{max}$ | $p_{min}$ | $p_{av}$ | $c^*$ |
| 1 | 0.929 | 0.580 | 0.065 | 0.065 | 0.190 | 0.766 | 0.483 | 0.370 | 0.169 | 0.269 | 0.112 |
| 2 | 0.387 | 0.963 | 0.340 | 0.236 | 0.533 | 0.724 | 0.314 | 0.566 | 0.538 | 0.552 | 0.353 |
| 3 | 0.524 | 0.954 | 0.353 | 0.263 | 0.558 | 0.760 | 0.326 | 0.572 | 0.536 | 0.554 | 0.370 |
| 4 | 0.771 | 0.806 | 0.187 | 0.148 | 0.348 | 0.751 | 0.392 | 0.477 | 0.350 | 0.414 | 0.232 |
| 5 | 0.523 | 0.949 | 0.523 | 0.156 | 0.397 | 0.562 | 0.124 | 0.778 | 0.736 | 0.757 | 0.551 |
| 6 | 0.340 | 0.991 | 0.648 | 0.262 | 0.545 | 0.627 | 0.124 | 0.802 | 0.793 | 0.797 | 0.654 |
| 7 | 0.121 | 0.997 | 0.648 | 0.255 | 0.565 | 0.625 | 0.122 | 0.805 | 0.803 | 0.804 | 0.650 |
| 8 | 0.620 | 0.841 | 0.170 | 0.089 | 0.342 | 0.668 | 0.304 | 0.545 | 0.439 | 0.492 | 0.202 |
| 9 | 0.829 | 0.783 | 0.140 | 0.084 | 0.317 | 0.711 | 0.342 | 0.520 | 0.379 | 0.449 | 0.179 |
| 10 | 0.223 | 0.942 | 0.460 | 0.225 | 0.284 | 0.492 | 0.209 | 0.575 | 0.518 | 0.547 | 0.488 |
| 11 | 0.248 | 0.945 | 0.510 | 0.230 | 0.295 | 0.488 | 0.181 | 0.628 | 0.571 | 0.600 | 0.540 |
| 12 | 0.875 | 0.780 | 0.090 | 0.107 | 0.394 | 0.840 | 0.519 | 0.382 | 0.267 | 0.325 | 0.115 |
| 13 | 0.815 | 0.820 | 0.150 | 0.087 | 0.384 | 0.743 | 0.330 | 0.556 | 0.438 | 0.497 | 0.183 |
| 14 | 0.719 | 0.823 | 0.170 | 0.105 | 0.338 | 0.699 | 0.339 | 0.515 | 0.398 | 0.456 | 0.207 |
| 15 | 0.543 | 0.933 | 0.374 | 0.220 | 0.515 | 0.743 | 0.269 | 0.638 | 0.583 | 0.610 | 0.401 |
| 16 | 0.840 | 0.807 | 0.229 | 0.174 | 0.352 | 0.761 | 0.369 | 0.515 | 0.376 | 0.445 | 0.284 |

[1]Soil clay content ($c$), relative volume of solids of contributive clay ($v_s$), relative volume of contributive clay in oven-dried state ($v_z$), oven-dried relative volume of the intra-aggregate matrix ($u_z$), relative volume of the non-clay solids ($u_S$), upper ($p_{max}$) and lower ($p_{min}$) boundaries of of the silt-sand grain porosity in the (imagined) contact state, average value of the porosity ($p_{av}$), and critical clay content ($c^*$).
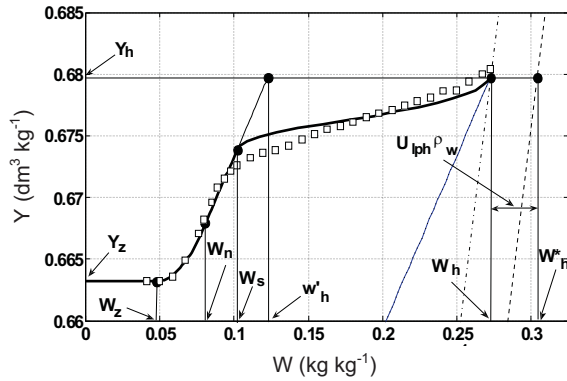
**Fig. 3.** Shrinkage curve data (white squares) and prediction (solid line) corresponding to soil 14 in Tables 1 and 2 and point 14 in Figs.2 and 5. The dotted line is parallel to the shrinkage curve in the basic shrinkage area. Dashed and dash-dot inclined lines are the true and pseudo saturation lines, respectively. The water contents $W_z$, $W_n$, $W_s$, $W_h$, and $W_h^*$, correspond to shrinkage limit, end-point of basic shrinkage, end-point of structural shrinkage, maximum swelling, and filling of lacunar pores (if they are filled in), respectively. The specific volumes $Y_z$ and $Y_h$ correspond to oven-dried state and maximum swelling, respectively. $w_h'$ is the maximum contribution of the intra-aggregate matrix to the total water content $W_h$ at maximum swelling. $U_{lph}=(W_h^*-W_h)/\rho_W$ is the specific volume of lacunar pores in the intra-aggregate matrix at maximum swelling.
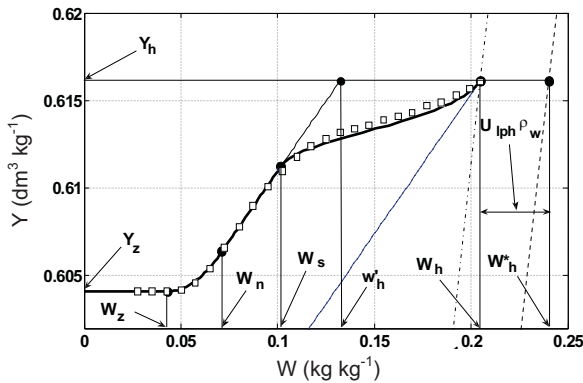


**Fig. 4.** Shrinkage curve data (white squares) and prediction (solid line) corresponding to soil 16 in Tables 1 and 2 and point 16 in Figs 2 and 5. Explanations as in Fig. 3.

## RESULTS AND DISCUSSION

The solid curve in Fig. 2 shows the theoretical dependency $k(c/c^*)$ from Eq. (14). Estimates of $c/c^*$ and $k$ for the sixteen soils from Table 2 are shown by the numbered points in Fig. 2 with the theoretical line. The numbers correspond to numbers of the soils in Tables 1 and 2. In Fig. 2 all the points are for values of $c/c^*>0.5$ although the clay content of the

soils varies in the wide range $0.065<c<0.648$ (Table 2). In this connection it is worth noting some obvious correlation between the $c$ values and found $c^*$ values of a soil (Table 2). This is why the soils with the relatively small clay content do not provide the information on $k(c/c^*)$ dependency at $c/c^*<0.5$. This fact was mentioned and used in the substantiation of Eq. (6) (see lines before Eq. (6)).

The experimental errors of $c/c^*$ and $k$ can be estimated as follows. The standard deviation $\delta c$ of $c$ is estimated, by order of magnitude, by the unit of a last decimal sign (Table 2): $\delta c \sim 0.001$. Accounting for the $c$ values in Table 2 $\delta c/c \leq 0.01\text{-}0.02$. Since $c^*$ correlates with $c$ (Table 2) for $\delta c^*/c^*$ we also have the similar estimate $\delta c^*/c^* \leq 0.01\text{-}0.02$. Then, denoting the standard deviation of $c/c^*$ by $D_c$ one has $D_c/(c/c^*) \cong |\delta c/c|+|\delta c^*/c^*| \leq 0.02\text{-}0.04$. That is, $D_c \leq (0.02\text{-}0.04)$ $(c/c^*)$. Furthermore, we can estimate the standard deviation of $k$ for a soil as $D_k \sim \delta S \cong S(|\delta a/a|+|\delta \beta/b|)S$ where: $S$ is the slope of the soil shrinkage curve in the basic shrinkage area ($k=1-S$, here we omitted $\rho_W$), $\delta S$ is its standard deviation, and $S=a/b$ ($a$ and $b$ are the vertical and horizontal projections of the linear section of the shrinkage curve at $W_n<W<W_s$; Figs 3 and 4). By order of magnitude the relative measurement accuracy of $a$ and $b$ values is $\delta a/a \sim \delta b/b \leq 0.01\text{-}0.02$. That is, $D_k \leq (0.02\text{-}0.04)S \leq (0.02\text{-}0.04)$ (because $S<1$). It is seen (Fig. 2) that the above standard deviations of the $c/c^*$ ratio, $D_c$ for the sixteen soils are appreciably smaller than the $c/c^*$ ratio variation $\Delta(c/c^*) \cong 0.5$ in the available range $0.5<c/c^*<1$: $D_c/\Delta(c/c^*)<<1$. The same is true for the $k$ factor in the available range $0<k<1$: $D_k/\Delta k \sim D_k<<1$. Hence, the available ranges of the experimental $c/c^*$ values and $k$ values are large enough to consider discrepancies between experimental points $(c/c^*, k)$ and the theoretical line in Fig. 2 as having statistical meaning. There are three possible sources for these discrepancies:

– approximations in the derivation of the theoretical line $k(c/c^*)$,
– measurement errors of the shrinkage curve,
– the procedure for counting the $v_s$ and $v_z$ parameters as well as estimating the porosity, $p$ of contacting grains through $p_{av}$.

Nevertheless, the above estimates of the experimental errors of $k$ and $c/c^*$ ($D_k$ and $D_c$) as well as the distribution of the points around the theoretical curve in Fig. 2 show that the discrepancies do not, as a rule, surpass two standard deviations along the $c/c^*$ and/or $k$ axes. Hence, one may say that, in spite of the approximations used, the predicted model line $k(c/c^*)$ and values estimated for sixteen soils from published data do agree.

The $k(c/c^*)$ dependence (Eq. (14)) can be practically written as $k^3=1-(c/c^*)^3$ also ie as a linear relation between $k^3$ and $(c/c^*)^3$. For this reason still another formal presentation of the $k(c/c^*)$ dependence is possible on the $((c/c^*)^3, k^3)$ plane. Figure 5 shows this presentation that is also convenient for the comparison between the theory and data. Note that the standard deviations of $k^3$ and $(c/c^*)^3$ are $\leq 3D_k$ and $\leq 3D_c$,
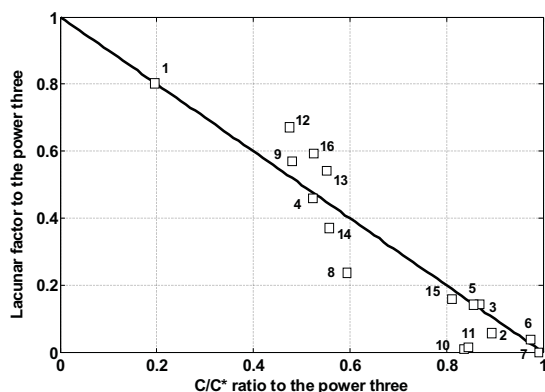
**Fig. 5.** Presentation of the theoretical dependence of $k(c/c^*)$ (solid line) and experimental data (white squares) in coordinates $x=(c/c^*)^3$, $y=k^3$ (the numbers refer to soils shown in Tables 1 and 2).

respectively. Accounting for that one can see that the discrepancies between the data and theory in Fig. 5 also do not exceed two standard deviations of $(c/c^*)^3$ and/or $k^3$.

The published works considering the reference shrinkage curve model contain the data analysis of the limited soil number: eight soils with sufficiently high clay content ($c/c^*>1$, $k=0$) (Chertkov, 2007a, b) and seven soils with sufficiently low clay content ($c/c^*<1$, $0<k<1$) (Chertkov, 2007c). The soils from 8 through 16 (Table 1) are of additional interest from this viewpoint allowing one to broaden this soil list. Figs 3 and 4 show examples of the comparison between experimental (Boivin *et al.*, 2006; Braudeau and Mohtar, 2004) and predicted (using the approach from Chertkov, 2007a, c) shrinkage curves for soils 14 and 16 from Table 1, respectively. Table 1 also shows the maximum relative difference $\delta=\max(|Y-Y_e|/Y_e)$ between the predicted ($Y$) and experimental ($Y_e$) values of the specific volume for the soils under consideration. One can see that in the majority cases the $\delta$ value is quite small and in any case is within the limits of experimental error.

## CONCLUSIONS

1. There were presented some consideration and results to show that the lacunar factor, as a fundamental property of aggregated soil with sufficiently small clay content, can be found independently of an experimental shrinkage curve based on a number of measured soil parameters.

2. A theoretical expression for lacunar factor as a function of the clay content to its critical value ratio was derived.

3. This expression was validated using available data on sixteen soils.

4. The measured physical soil parameters for finding the lacunar factor are: soil clay content ($c$); porosity of the silt and sand grains (contributing the soil) in the (imagined) contact state ($p$); relative volume of solids of contributive clay ($v_s$); and relative volume of contributive clay in the oven-dried state ($v_z$).

5. The analysis in the work allowed the supplementary substantiation of the reference shrinkage curve model on the data of new soils.

## REFERENCES

**Boivin P., Garnier P., and Vauclin M., 2006.** Modeling the soil shrinkage and water retention curves with the same equations. Soil Sci. Soc. of Am. J., 70, 1082-1093.

**Braudeau E., Costantini J.M., Bellier G., and Colleuille H., 1999.** New device and method for soil shrinkage curve measurement and characterization. Soil Sci. Soc. Am. J., 63, 525-535.

**Braudeau E., Frangi J-P., and Mohtar R.H., 2004.** Characterizing nonrigid aggregated soil-water medium using its shrinkage curve. Soil Sci. Soc. Am. J., 68, 359-370.

**Braudeau E. and Mohtar R.H., 2004.** Water potential in nonrigid unsaturated soil-water medium. Water Resour. Res., 40, W05108, doi:10.1029/2004WR003119.

**Braudeau E., Sene M., and Mohtar R.H., 2005.** Hydrostructural characteristics of two African tropical soils. Eur. J. Soil Sci., 56, 375-388.

**Cabidoche Y-M. and Ruy S., 2001.** Field shrinkage curves of a swelling clay soil: analysis of multiple structural swelling and shrinkage phases in the prisms of a Vertisol. Aust. J. Soil Res., 39, 143-160.

**Chertkov V.Y., 2000.** Modeling the pore structure and shrinkage curve of soil clay matrix. Geoderma, 95, 215-246.

**Chertkov V.Y., 2003.** Modeling the shrinkage curve of soil clay pastes. Geoderma, 112, 71-95.

**Chertkov V.Y., 2005.** Intersecting-surfaces approach to soil structure. Int. Agrophysics, 19, 109-118.

**Chertkov V.Y., 2007a.** The reference shrinkage curve at higher than critical soil clay content. Soil Sci. Soc. Am. J., 71(3), 641-655.

**Chertkov V.Y., 2007b.** The reference shrinkage curve of clay soil. Theor. Appl. Fracture Mechanics, 48(1), 50-67.

**Chertkov V.Y., 2007c.** The soil reference shrinkage curve. Open Hydrology J., 1, 1-18.

**Chertkov V.Y., 2008a.** The physical effects of an intra-aggregate structure on soil shrinkage. Geoderma, 146, 147-156.

**Chertkov V.Y., 2008b.** The geometry of soil crack networks. Open Hydrology J., 2, 34-48.

**Chertkov V.Y., 2008c.** Using the reference shrinkage curve to estimate the corrected crack volume of a soil layer. Open Mechanics J., 2, 21-27.

**Chertkov V.Y., 2008d.** Estimating the aggregate/intraaggregate mass ratio of a shrinking soil. Open Hydrology J., 2, 7-14.

**Cornelis W.M., Corluy J., Medina H., Hartmann R., Van Meir-venne M., and Ruiz M.E., 2006.** A simplified parametric model to describe the magnitude and geometry of soil shrinkage. Eur. J. Soil Sci., 57, 258-268.

**Crescimanno G. and Provenzano G., 1999.** Soil shrinkage characteristic curve in clay soils: Measurement and prediction. Soil Sci. Soc. Am. J., 63, 25-32.

**Giraldez J.V., Sposito G., and Delgado C., 1983.** A general soil volume change equation: I. The two-parameter model. Soil Sci. Soc. Am. J., 47, 419-422.

**Groenevelt P.H. and Bolt G.H., 1972.** Water retention in soil. Soil Sci., 113(4), 238-245.

**Groenevelt P.H. and Grant C.D., 2001.** Re-evaluation of the structural properties of some British swelling soils. Eur. J. Soil Sci., 52, 469-477.

**McGarry D. and Daniels I.J., 1987.** Shrinkage curve indices to quantify cultivation effects of soil structure of a Vertisol. Soil Sci. Soc. Am. J., 51, 1575-1580.

**Olsen P.A. and Haugen L.E., 1998.** A new model of the shrinkage characteristics applied to some Norwegian soils. Geoderma, 83, 67-81.

**Peng X. and Horn R., 2005.** Modeling soil shrinkage curve across a wide range of soil types. Soil Sci. Soc. Am. J., 69, 584-592.

**Sander T. and Gerke H.H., 2007.** Noncontact shrinkage curve determination for soil clods and aggregates by three-dimensional optical scanning. Soil Sci. Soc. Am. J., 71, 1448-1454.

**Tariq A.-R. and Durnford D.S., 1993.** Analytical volume change model for swelling clay soils. Soil Sci. Soc. Am. J., 57, 1183-1187.

**Yule D.F. and Ritchie J.T., 1980a.** Soil shrinkage relationships of Texas Vertisols: I. Small cores. Soil Sci. Soc. Am. J., 44, 1285-1291.

**Yule D.F. and Ritchie J.T., 1980b.** Soil shrinkage relationships of Texas vertisols: I. Large cores. Soil Sci. Soc. Am. J., 44, 1291-1295.